Responsive mechanism of 2-(2′-hydroxyphenyl)benzoxazole-based two-photon fluorescent probes for zinc and hydroxide ions*

Zhang Yu-Jin(张玉瑾), Zhang Qiu-Yue(张秋月), Ding Hong-Juan(丁红娟), Song Xiu-Neng(宋秀能), and Wang Chuan-Kui(王传奎)†

College of Physics and Electronics, Shandong Normal University, Jinan 250014, *China*

(Received 1 June 2014; revised manuscript received 24 September 2014; published online 10 December 2014)

Response theory is used to investigate one- and two-photon absorption (TPA) as well as the emission properties of a series of potential zinc ion and pH sensitive materials containing 2-(2′-hydroxyphenyl)benzoxazole (HPBO) end groups. Special emphasis is placed on the evolution of their optical properties upon combining with zinc ions or deprotonation. Our calculated results indicate that upon combining with zinc ions or deprotonation, these HPBO derivatives show drastic changes in their one-photon absorption (OPA), emission, and TPA properties. Moreover, the mechanisms of the probes are analyzed and found to be an intramolecular charge transfer. These compounds are thus proved to be excellent candidates for two-photon fluorescent zinc and pH probes.

Keywords: two-photon absorption, response theory, zinc probe, pH probe

PACS: 33.80.Wz, 31.70.Dk, 31.15.A– **DOI:** 10.1088/1674-1056/24/2/023301

1. Introduction

Materials with large two-photon absorption (TPA) cross sections are expected to have potential applications in many fields, such as three-dimensional (3D) optical data storage,[1–3] photodynamic therapy,[4–7] optical limiting,[8–11] and two-photon excitation microscopy (TPEM) imaging.[12–15] Especially, the TPEM imaging has received extensive attention in recent years because of its vital uses in the study of living cells and tissues, which has many advantages over the commonly used one-photon excitation microscopy (OPEM) imaging, including reducing photodamage and photobleaching, increasing the penetration depth, dark-field imaging, and high 3D resolution. Certainly, utilizations of the TPEM imaging rely on the development of efficient TPA materials. Moreover, a powerful two-photon fluorescent (TPF) probe needs to have a large TPA cross section, appreciable solubility in water, high photostability, and sensitive response to detected objects. Over the past decade, TPF probes triggered by diverse external stimuli, such as metal ions, pH values, and fluoride ions, have been experimentally developed.[16–20] At the same time, working mechanisms of the probes, including intramolecular charge transfer (ICT), fluorescence resonance energy transfer (FRET), photoinduced electron transfer (PET), and group conversion (GC), have also been discussed.[21]

2-(2′-hydroxyphenyl)benzoxazole (HPBO)-containing materials are promising candidates for zinc ion probes and pH probes because the HPBO part can be chelated with zinc ions to form a zinc complex and they can also be deprotonated to form a free phenolate anion in an alkaline environment. Various one-photon fluorescent (OPF) sensing 2-(2′-hydroxyphenyl)benzoxazole (HPBO) derivatives have been developed for selective detection of zinc ions in environmental or biological systems.[22–25] Recently, zinc ion and pH probes based on TPA chromophores with HPBO groups have been reported, in which three HPBO-based chromophores have been synthesized and investigated, revealing them as potential probes for zinc and hydroxide ions.[19] However, to the best of our knowledge, theoretical investigations on these TPF-based probes are quite limited. In order to understand the responsive mechanisms of these probes, theoretical investigations of their TPA and fluorescent properties by the response theory methods at the density functional theory (DFT) level will be carried out in this work. Our study is intended to give the working mechanisms and structure-property relationships for these probes, providing knowledge that can be used to design more efficient TPF probes that are geared towards biological applications.

2. Computational details

The one-photon absorption (OPA) strength between ground state $|i\rangle$ and excited state $|f\rangle$ is described by the oscillator strength

$$\delta_{\mathrm{op}} = \frac{2\omega_f}{3}\sum_{\alpha}|\langle i|\mu_\alpha|f\rangle|^2, \tag{1}$$

where ω_f is the excited energy and μ_α is the Cartesian component of the electronic dipole moment operator. The summation

*Project supported by the National Basic Research Program of China (Grant No. 2011CB808105) and the National Natural Science Foundation of China (Grant No. 21303096).

†Corresponding author. E-mail: ckwang@sdnu.edu.cn

© 2015 Chinese Physical Society and IOP Publishing Ltd

is performed over the molecular x, y, and z axes: $\alpha \in \{x,y,z\}$.

The TPA cross section that can be directly compared with experimental result is defined as

$$\sigma_{\rm tp} = \frac{4\pi^2 a_0^5 \alpha \omega^2 g(\omega)}{15 c_0 \Gamma} \delta_{\rm tp}. \quad (2)$$

Here α_0 is the Bohr radius, c_0 is the speed of the light in vacuum, α is the fine structure constant, ω is the photon frequency of an incident laser beam, $g(\omega)$ is the spectrum line profile and is assumed to be a δ function here, Γ is the lifetime broadening of the final state and is assumed to a common value 0.1 eV, and $\delta_{\rm tp}$ is the microscopic TPA cross section that is defined by a two-photon transition matrix element $S_{\alpha\beta}$ between the initial state $|i\rangle$ and the final state $|f\rangle$

$$S_{\alpha\beta} = \sum_s \left[\frac{\langle i|\mu_\alpha|s\rangle\langle s|\mu_\beta|f\rangle}{\omega_{\rm si} - \omega} + \frac{\langle i|\mu_\beta|s\rangle\langle s|\mu_\alpha|f\rangle}{\omega_{\rm si} - \omega} \right]. \quad (3)$$

Here, $\alpha, \beta \in \{x,y,z\}$; ω is the photon frequency of an incident laser beam and is assumed to be half of the excitation energy ω_f of the final state $|f\rangle$, $2\omega = \omega_f$; the summation covers all of the intermediate states including states $|i\rangle$ and $|f\rangle$; $\omega_{\rm si}$ represents the excited energy of the intermediate state $|s\rangle$. The microscopic TPA cross section of the molecule excited by a linearly polarized monochromatic beam can be calculated by

$$\begin{aligned}\delta_{\rm tp} &= 6(S_{xx}+S_{yy}+S_{zz})^2 \\ &\quad +8\left(S_{xy}^2+S_{xz}^2+S_{yz}^2-S_{xx}S_{yy}-S_{xx}S_{zz}-S_{yy}S_{zz}\right). \quad (4)\end{aligned}$$

The most straightforward approach to calculating the TPA cross section is the response theory method. In this theory, the summation over excited states is substituted by the solution of a set of coupled response equations. TPA transition matrix elements can be obtained from the residue of the quadratic response function. In this study, the geometrical structures of ground state are fully optimized at a Hartree–Fock (HF) level. Frequency calculations are performed to verify the stability of the optimized structures at the same level. On the basis of each optimized ground state structure, OPA and TPA properties are calculated by using the response theory method that is implemented in Dalton2011 package[26] at the DFT/B3LYP level. The emission properties are also obtained by the response theory method at the DFT/B3LYP level after optimizing the first excited state structures with time-dependent hybrid density functional theory (TD-DFT). All of the optimizations of geometrical structures are implemented in Gaussian09 package.[27] The basis set 6-31G* is chosen for the study. For the purpose of simulating the deprotonation of hydroxyl end groups, a hydrogen atom attached to an oxygen atom in the hydroxyl group is removed and an electron in the molecule is simultaneously left there. The most part of the electron charge is held by the oxygen atom because of its high electronegative property. Furthermore, solvent effects caused by the surrounding DMF solvent are taken into account in the polarized continuum model (PCM) approach[28,29] for comparison with the experimental results. The charge transfer (CT) process is visualized to understand their optical properties.

3. Results and discussion

3.1. Molecular structures

The molecular structures are presented in Fig. 1. For the purpose of saving computational resources, we replace the aliphatic side chains ($-C_6H_{13}$) in the fluorene center by a hydrogen atom, and the end group ($-OC_6H_{13}$) of the molecule 2 by a smaller one ($-OC_2H_5$). One can expect that this substitution can significantly reduce the computational cost and has little effect on nonlinear optical properties of the compounds used in experiment. All of the the studied molecules have fluorenes as π centers. Molecules 1, 2, and 3 contain HPBO groups with an increasing number (0, 1, and 2) as binding sites for metal ions, respectively. Complexes 2–Zn and 3–Zn are in saturated states of zinc ions because the molecules 2 and 3 are titrated with $Zn(OOCCH_3)_2$ solvent. Molecule 3–O^- is a twofold deprotonated form of molecule 3.

Some selective bond lengths and dihedral angles of the optimized molecules are displayed in Table 1. When compounds 2 and 3 are chelated with zinc ions to form the zinc complexes 2–Zn and 3–Zn, their bond lengths of C_7–O_{11} are contracted from 1.331 Å to 1.283 Å, showing the larger electron donating ability of the terminal group –OZn. As the compound 3 is deprotonated to form the twofold deprotonated form 3–O^-, the bond length of C_7–O_{11} is contracted from 1.331 Å to 1.225 Å, enhancing the electron donating ability of the hydroxyl group after deprotonation. Additionally, the bond length alternation (BLA) parameters defined by $d_{\rm BLA} = (R_{C_2-C_3} + R_{C_4-C_5})/2 - R_{C_3-C_4}$ are 0.148, 0.148, 0.146, 0.148, 0.146, and 0.126 Å for the compounds 1, 2, 2–Zn, 3, 3–Zn, and 3–O^-, respectively. We can find that the BLA values of the zinc complexes 2–Zn and 3–Zn as well as the deprotonated 3–O^- are reduced, which indicates that the conjugated degrees of these HPBO derivatives are increased upon combining with zinc ions or deprotonation. Besides, the dihedral angles between the center fluorene plane and the HPBO group of 1, 2, and 3 ($\angle C_1C_2C_5C_6$) are 48.53°, 44.83°, and 44.76°, respectively. We can see that the optimized structures of compounds 1, 2, and 3 are not in good planarity, but the planarity is a little improved as the number of HPBO units increases. After combining with zinc ions and deprotonation, 2–Zn, 3–Zn, and 3–O^- have better planarity with the dihedral angles $\angle C_1C_2C_5C_6$ of 38.61°, 39.01°, and 18.93°, respectively.

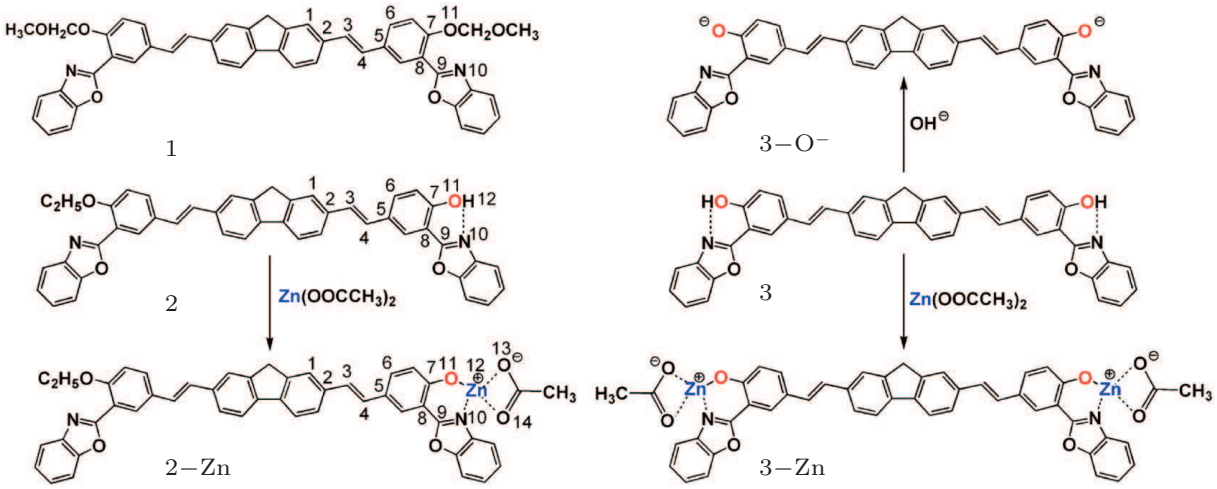


Fig. 1. (color online) Molecular structures of all the HPBO-containing compounds.

Table 1. Selective bond lengths (in units of Å) and dihedral angles (in units of C^0) of the optimized chromophores.

	1	2	2–Zn	3	3–Zn	3–O$^-$
C_2–C_3	1.477	1.477	1.477	1.477	1.477	1.473
C_3–C_4	1.328	1.328	1.329	1.328	1.329	1.338
C_4–C_5	1.476	1.475	1.473	1.475	1.473	1.456
C_8–C_{19}	1.472	1.459	1.442	1.459	1.442	1.444
C_7–O_{11}	1.337	1.331	1.283	1.331	1.283	1.225
O_{11}– Zn_{12}/H_{12}	–	0.957	1.886	0.957	1.886	–
Zn_{12}/H_{12}–N_{10}	–	1.912	2.024	1.912	2.024	–
Zn_{12}–O_{13}	–	–	2.042	–	2.042	–
Zn_{12}–O_{14}	–	–	2.041	–	2.042	–
$\angle C_1C_2C_5C_6$	48.53	44.83	38.61	44.76	39.01	18.93

The charge distribution of the chromophores is an important factor for determining their photophysical properties. We thus perform a Mulliken population analysis on free molecules 1, 2, and 3 and their ion forms. To make a clear analysis, these molecules are divided into five parts, as shown in Fig. 2. Parts A and C act as the terminal donors/acceptors of the molecule, part B acts as the conjugate bridge of the molecule, and parts D and E represent the benzoxazole units. The net charges of these parts are listed in Table 2. From Table 2, one can see that Q_D and Q_E values of the molecules except for the complex 3–O$^-$ are near to zero, which demonstrates that the benzoxazole units are not directly conjugated with the rest of the chromophore. Q_D and Q_E values of the complex 3–O$^-$ are due to the deprotonated process. It is noteworthy that all of the terminal groups, –OCH$_2R$ (R = OCH$_3$ for 1 and CH$_3$ for 2), –OH, –OZn, and –O$^-$, possess a considerable number of electrons, showing a donating ability to the π–center. When compound 2 combines with a zinc ion, Q_A (Q_C) is increased from $-0.201e$ ($-0.204e$) to $-0.257e$ ($-0.267e$), and for compound 3, Q_A is increased from $-0.204e$ to $-0.268e$. When compound 3 is deprotonated, the value of Q_A is $-0.657e$. These results show that charge push–pull capabilities of these HPBO-based molecules are enhanced by combining with zinc ions or deprotonation.

Table 2. Net charges (in units of e) for divided parts of the chromophores in the ground state.

Molecule	Q_A	Q_B	Q_C	Q_D	Q_E
1	–0.222	0.559	–0.222	–0.057	–0.057
2	–0.201	0.540	–0.204	–0.063	–0.071
2–Zn	–0.257	0.644	–0.267	–0.060	–0.058
3	–0.204	0.551	–0.204	–0.071	–0.071
3–Zn	–0.268	0.655	–0.268	–0.059	–0.059
3–O$^-$	–0.657	–0.203	–0.657	–0.241	–0.241

The frontier orbital energies and energy gaps (ΔE_{H-L}) between the highest occupied molecular orbital (HOMO) and the lowest unoccupied molecular orbital (LUMO) are shown in Table 3. The ΔE_{H-L} values of molecules 2 and 3 reduce to 3.62 eV compared with that of molecule 1 (3.65 eV) owing to the introduction of HPBOs. When zinc ions are added, the HOMO energy moves up and LUMO energy moves down, resulting in a narrower energy gap. Furthermore, the ΔE_{H-L} value of 2.68 eV for the deprotonated 3–O$^-$ is smallest. This observation is understandable because the charge push-pull abilities of the chromophores 2–Zn, 3–Zn, and 3–O$^-$ are stronger than those of the free forms.

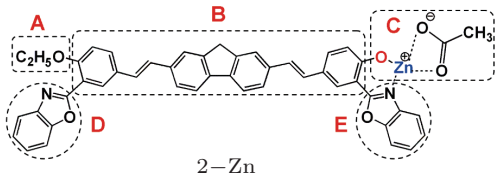


Fig. 2. (color online) Five divided parts of the molecule 2–Zn.

Table 3. Calculated frontier orbital energies (in units of eV). H (L) denotes the HOMO (LUMO).

Molecule	H–3	H–2	H–1	H	L	L+1	L+2	L+3	ΔE_{H-L}
1	–6.13	–5.94	–5.60	–5.14	–1.49	–1.15	–1.04	–0.70	3.65
2	–6.27	–5.97	–5.53	–5.07	–1.45	–1.34	–1.11	–0.69	3.62
2–Zn	–6.38	–6.09	–5.58	–5.02	–1.63	–1.47	–1.14	–0.72	3.39
3	–6.38	–6.12	–5.56	–5.08	–1.46	–1.37	–1.31	–0.73	3.62
3–Zn	–6.52	–5.99	–5.28	–4.88	–1.60	–1.61	–1.29	–0.61	3.27
3–O^-	–1.32	–1.32	–0.36	–0.16	2.52	3.01	3.07	3.36	2.68

3.2. One-photon absorption and emission properties

The calculated OPA and emission properties, including the maximum OPA wavelength (λ^{O}_{max}), emission wavelength (λ^{E}_{max}), transition energy (E_{flu}), oscillator strength (δ_{op}), transition nature, emission lifetime (τ), and experimental results, are listed in Table 4. The maximum OPA peaks of compounds 1, 2, and 3 in gas phase are located at 375, 377, and 376 nm, respectively. When the solvent effect is considered, these peaks are red-shifted to 380, 383, and 381 nm, showing that they are in good agreement with the experimental measurements of 382, 381, and 384 nm. The results with considering solvent effect are included in the following discussion. When molecules 2 and 3 bind to zinc ions, their maximum values of OPA wavelength λ^{O}_{max} and emission wavelength λ^{E}_{max} each have a significant red-shift. Namely, $\lambda^{O}_{max}(\lambda^{E}_{max})$ of 2 and 2–Zn are, respectively, 383 nm (494 nm) and 398 nm (505 nm), and those of 3 and 3–Zn are respective 381 nm (493 nm) and 401 nm (518 nm), showing that they are in good agreement with the experimental measurements. Furthermore, one can see that the emission intensities of 2–Zn and 3–Zn are largely reduced. These variations can be used to indicate the presence of zinc ions. When molecule 3 is deprotonated, λ^{O}_{max} is red-shifted from 381 nm to 464 nm, and λ^{E}_{max} is also red-shifted from 493 nm to 546 nm. Nevertheless, the emission intensity of 3–O^- is enhanced. The results indicate that molecule 3 may serve as a pH probe.

The emission lifetime τ is further calculated by using the Einstein transition properties according to the formula (in a.u.)

$$\tau = \frac{c^3}{2(E_{flu})^2 \delta_{op}}, \tag{5}$$

where c is the velocity of light, E_{flu} is the transition energy, and δ_{op} is the oscillator strength. Complex 3–Zn has a longest emission lifetime of 15.78 ns, and the next one is 2–Zn with an emission lifetime of 7.50 ns, which are much larger than those of the free molecules and 3–O^-.

Table 4. One-photon absorption and emission properties of the chromophores for the charge transfer state in the lower energy region.

Molecule	λ^{O}_{max}/nm	δ_{op}	Transition nature	λ^{E}_{max}/nm	E_{flu}/eV	δ_{op}	Transition nature	τ/ns
1	375 380[a] 382[b]	2.40	$S_0 \rightarrow S_1$ H→L 86%	473 491[a] 442[b]	2.62	2.82	$S_1 \rightarrow S_0$ H→L 99%	1.19
		2.46	$S_0 \rightarrow S_1$ H→L 88%		2.52	2.91	$S_1 \rightarrow S_0$ H→L 99%	1.25
2	377 383[a] 381[b]	2.27	$S_0 \rightarrow S_1$ H→L 92%	477 494[a] 494[b]	2.60	2.76	$S_1 \rightarrow S_0$ H→L 98%	1.23
		2.49	$S_0 \rightarrow S_1$ H→L 93%		2.51	2.89	$S_1 \rightarrow S_0$ H→L 99%	1.27
2–Zn	385 398[a] 394[b]	1.98	$S_0 \rightarrow S_2$ H→L+1 95%	538 505[a] 500[b]	2.30	0.18	$S_1 \rightarrow S_0$ H→L 99%	24.18
		1.91	$S_0 \rightarrow S_1$ H→L 72%		2.45	0.51	$S_1 \rightarrow S_0$ H→L 97%	7.50
3	376 381[a] 384[b]	2.14	$S_0 \rightarrow S_1$ H→L 83%	475 493[a] 499[b]	2.61	2.93	$S_1 \rightarrow S_0$ H→L 98%	1.15
		2.44	$S_0 \rightarrow S_1$ H→L 92%		2.51	3.07	$S_1 \rightarrow S_0$ H→L 98%	1.18
3–Zn	384 401[a] 403[b]	2.59	$S_0 \rightarrow S_3$ H→L+2 94%	557 518[a] 500[b]	2.22	0.12	$S_1 \rightarrow S_0$ H→L 98%	38.93
		1.65	$S_0 \rightarrow S_1$ H→L 55%		2.39	0.25	$S_1 \rightarrow S_0$ H→L 95%	15.78
3–O^-	517 464[a] 441[b]	2.33	$S_0 \rightarrow S_1$ H→L 88%	575 546[a] 540[b]	2.15	2.89	$S_1 \rightarrow S_0$ H→L 97%	1.72
		2.67	$S_0 \rightarrow S_1$ H→L 89%		2.27	3.17	$S_1 \rightarrow S_0$ H→L 95%	1.41

[a]In DMF, [b]experimental results.[19]

As is well known, optical properties strongly depend on the intramolecular charge transfer (ICT). The charges in a molecule will redistribute when the molecule is excited from the ground state to the excited state. In order to obtain a better understanding of the ICT process, we plot the charge density difference between the ground state and the first excited state (see Fig. 3). From Fig. 3, one can see that there exists a local charge transfer in HPBO group, namely, electrons transfer from hydroxyphenyl to benzoxazole for the free molecules. Molecules 1, 2, and 3 are observed as a typical D–π–D configuration, and their optical properties are determined by the donating ability of the terminal group. The process combining

zinc ions or deprotonating enhances electron donating capabilities of the terminal groups, which further leads to change of electronic structure of the molecules. As a result, their optical absorption and emission properties are modulated. It is shown in Fig. 3 that the charge transfer profile has a considerable change upon combining with zinc ions or deprotonation. Charge transfer in the complex 3–Zn from the end substituents to the π-center is enhanced, while the electrons in 2–Zn are transferred from the –OZn group to the other side, showing a dipolar characteristic. Upon deprotonation, charge transfer in the complex 3–O^- is very intensive, owing to the strong donor –O^-. The electron donating abilities of the terminal groups are deduced to be in the order of –O^- >–OZn>–OH/–OCH_2R. The intramolecular charge transfer is thus recognized to be the mechanism of the probe.

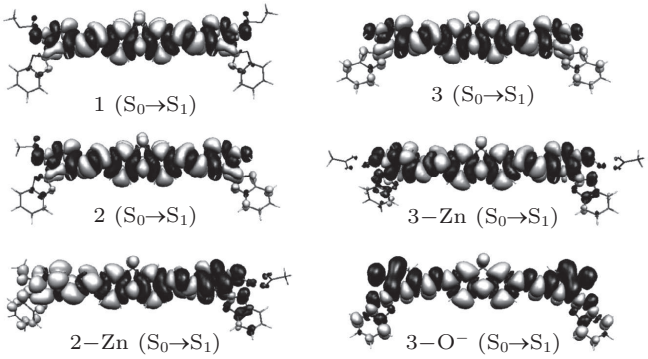


Fig. 3. Charge variations between charge transfer states and ground states of each molecule. The white and black areas represent electron gain and loss, respectively.

3.3. Two-photon absorption properties

The calculated TPA properties, including TPA cross sections and the corresponding TPA wavelengths of the lowest six excited states in DMF solvent, are shown in Table 5. The maximum TPA cross sections for free molecules 1, 2, and 3 are 3885 GM, 5400 GM, and 5614 GM (1 GM = 10^{-50} cm^4·s/photon), which are located at 640 nm, 647 nm, and 647 nm, respectively. It is seen that TPA abilities are enlarged with the increase of the number of the HPBO groups, which shows the same trend as the experimental measurement.

When free molecules are combined with zinc ions and deprotonated, both the values and the location of the maximum TPA cross sections have an obvious variation. The maximum TPA cross section of 2–Zn is reduced to 4337 GM, which is in agreement with the experimental result. The reduction is possibly attributed to the molecular electrical change, in which molecule 2 is changed from a quadripolar system to a dipolar one after bonding with the zinc ion. Generally speaking, the TPA ability of a quadripolar compound is better than that of a dipolar compound.[30] The maximum TPA cross section of 3–Zn is 6052 GM at 673 nm, which is larger than that of molecule 3. When free molecule 3 is deprotonated, the maximum TPA cross section of 3–O^- takes the largest value of 6338 GM at 824 nm. This results from the enhanced electron donating ability of the terminal groups as the hydroxy form (–OH) is transformed into the phenolated form (–O^-). In short, HPBO-containing compounds 2 and 3 can be used as TPF probes for zinc ions and pH.

Table 5. TPA cross sections σ_{tp} (GM = 10^{-50} $cm^4 \cdot s$/photon) and TPA wavelengths λ_{tp} (nm) of the lowest six excited states in a DMF solvent.

Molecule	λ_{tp}/nm	σ_{tp}/GM	Molecule	λ_{tp}/nm	σ_{tp}/GM
1	760	1	3	762	4
	694	660		725	100
	683	15		723	25
	640	3885		647	5614
	609	457		629	0
	603	0		627	366
		120[a]			530[a]
2	766	3	3–Zn	803	34
	727	78		794	54
	700	242		777	10
	647	5400		706	187
	630	199		704	36
	615	101		673	6052
		430[a]			470[a]
2–Zn	797	56	3–O^-	928	1
	777	748		824	6338
	696	257		790	4293
	657	440		782	201
	652	4337		718	3
	616	625		710	324
		270[a]			4120[a]

[a]Experimental results.[19]

4. Summary

The OPA, emission, and TPA properties of 2-(2′-hydroxyphenyl)benzoxazole- containing chromophores are theoretically studied at the DFT level. The mechanisms of the zinc ions and pH probes are analyzed. When the free molecules are combined with zinc ions and deprotonated, their BLA values are reduced and their terminal groups show enhanced electron donating capabilities. Both the maximum OPA wavelengths and emission wavelengths show drastic red shifts when combining with zinc ions or deprotonation takes place, and the complex 3–Zn has a longest emission lifetime of 15.78 ns. TPA abilities are enlarged as the number of HPBO groups increases, which shows the same trend as the experimental measurement. Both the values and the locations of the maximum TPA cross sections each have an obvious variation as the free molecules bind to zinc ions and molecule 3 is deprotonated. Overall, the molecules containing HPBO groups are proven to be sensitive to zinc ions as well as pH values,

and their recognition mechanism is the intramolecular charge transfer. These results suggest that these compounds are excellent candidates for two-photon zinc ion and pH probes.

References

[1] Corredor C C, Huang Z L, Belfield K D, Morales A R and Bondar M V 2007 *Chem. Mater.* **19** 5165

[2] Ogawa K and Kobuke Y 2009 *Org. Biomol. Chem.* **7** 2241

[3] Zhou H P, Zhou F X, Tang S Y, Wu P, Chen Y X, Tu Y L, Wu J Y and Tian Y P 2012 *Dyes and Pigments* **92** 633

[4] Balaz M, Collins H A, Dahlstedt E and Anderson H L 2009 *Org. Biomol. Chem.* **7** 874

[5] Boca S C, Four M, Bonne A, Sanden B V D, Astilean S, Baldeck P L and Lemercier G 2009 *Chem. Commun.* **45** 90

[6] Gallavardin T, Maurin M, Marotte S, Simon T, Gabudean A M, Bretonnière Y, Lindgren M, Lerouge F, Baldeck P L, Stéphan O, Leverrier Y, Marvel J, Parola S, Maury O and Andraud C 2011 *Photochem. Photobiol. Sci.* **10** 1216

[7] Shen X, Li L, Wu H, Yao S Q and Xu Q H 2011 *Nanoscale* **3** 5140

[8] Miao Q, Zhao P, Sun Y P, Liu J C and Wang C K 2009 *Acta Phys. Sin.* **58** 5455 (in Chinese)

[9] Sun Y P, Liu J C and Wang C K 2009 *Acta Phys. Sin.* **58** 3934 (in Chinese)

[10] Lin T C, Huang Y J, Chen Y F and Hu C L 2010 *Tetrahedron* **66** 1375

[11] Four M, Riehl D, Mongin O, Blanchard-Desce M, Lawson-Daku L M, Moreau J, Chauvin J, Delaire J A and Lemercier G 2011 *Phys. Chem. Chem. Phys.* **13** 17304

[12] Wang Y C, Zhou H, Ding J L, Chen Q, Xiao H B, Tao X M and Qian S X 2010 *Chin. Phys. Lett.* **27** 038201

[13] Zhu M Q, Zhang G F, Li C, Aldred M P, Chang E, Drezek R A and Li A D Q 2010 *J. Am. Chem. Soc.* **133** 365

[14] Han G C, Zhao K, Liu P W and Zhang L L 2012 *Chin. Phys. B* **21** 118201

[15] Luo Z, Yang B, Zhong C, Tang F, Yuan M, Xue Y, Yao G, Zhang J and Zhang Y 2013 *Dyes and Pigments* **97** 52

[16] Sumalekshmy S and Fahrni C J 2011 *Chem. Mater.* **23** 483

[17] Werts M H V, Gmouh S, Mongin O, Pons T and Blanchard-Desce M 2004 *J. Am. Chem. Soc.* **126** 16294

[18] Liu L, Zhou Z, Shi J, Liu Z, Lu C, He W, Ma J, Cui Y and Lu G Y 2011 *Synth. Met.* **161** 783

[19] Tian Y, Chen C Y, Yang C C, Young A C, Jang S H, Chen W C and Jen A K Y 2008 *Chem. Mater.* **20** 1977

[20] Zhang M, Li M, Li F, Cheng Y, Zhang J, Yi T and Huang C 2008 *Dyes and Pigments* **77** 408

[21] Huang C B, Yi D S, Feng C H, Ren A X and Sun S G 2010 *Prog. Chem.* **22** 2408 (in Chinese)

[22] Taki M, Wolford J L and O'Halloran T V 2004 *J. Am. Chem. Soc.* **126** 712

[23] Tong H, Zhou G, Wang L, Jing X, Wang F and Zhang J 2003 *Tetrahedron Lett.* **44** 131

[24] Ohshima A, Momotake A and Arai T 2004 *Tetrahedron Lett.* **45** 9377

[25] Yang C C, Tian Y, Chen C Y, Jen A K Y and Chen W C 2007 *Macromol. Rapid Commun.* **28** 894

[26] DALTON 2011 *A Molecular Electronic Structure Program*, Release Dalton2011, see http://daltonprogram.org/

[27] GAUSSIAN 09, References in http://www.gaussian.com/

[28] Fortunelli A and Tomasi J 1994 *Chem. Phys. Lett.* **231** 34

[29] Frediani L, Rinkevicius Z and Ågren H 2005 *J. Chem. Phys.* **122** 244104

[30] Wang C K, Macak P, Luo Y and Ågren H 2001 *J. Chem. Phys.* **114** 9813